Cork Open Research Archive
Cartlann Taighde Oscailte Chorcaí

UCC Library and UCC researchers have made this item openly available. Please let us know how this has helped you. Thanks!

Title	Low effective surface recombination in In(Ga)As/GaAs quantum dot diodes
Author(s)	Tanriseven, Selim; Corbett, Brian M.
Publication date	2011
Original citation	Tanriseven, S. and Corbett, B. (2011) 'Low effective surface recombination in In(Ga)As/GaAs quantum dot diodes', Journal of Applied Physics, 110(3), 034508 (5pp). doi: 10.1063/1.3611387
Type of publication	Article (peer-reviewed)
Link to publisher's version	http://aip.scitation.org/doi/10.1063/1.3611387 http://dx.doi.org/10.1063/1.3611387 Access to the full text of the published version may require a subscription.
Rights	**© 2011, American Institute of Physics. This article may be downloaded for personal use only. Any other use requires prior permission of the author and AIP Publishing. The following article appeared in Tanriseven, S. and Corbett, B. (2011) 'Low effective surface recombination in In(Ga)As/GaAs quantum dot diodes', Journal of Applied Physics, 110(3), 034508 (5pp). doi: 10.1063/1.3611387 and may be found at http://aip.scitation.org/doi/10.1063/1.3611387**
Item downloaded from	http://hdl.handle.net/10468/4736

Downloaded on 2021-04-19T08:33:51Z

University College Cork, Ireland
Coláiste na hOllscoile Corcaigh

.

Low effective surface recombination in In(Ga)As/GaAs quantum dot diodes

Selim Tanriseven and Brian Corbett

Citation: Journal of Applied Physics **110**, 034508 (2011); doi: 10.1063/1.3611387
View online: http://dx.doi.org/10.1063/1.3611387
View Table of Contents: http://aip.scitation.org/toc/jap/110/3
Published by the American Institute of Physics

AIP | Journal of Applied Physics
Save your money for your research.
It's now FREE to publish with us -
no page, color or publication charges apply.
Publish your research in the
Journal of Applied Physics
to claim your place in applied
physics history.

Low effective surface recombination in In(Ga)As/GaAs quantum dot diodes

Selim Tanriseven and Brian Corbett[a]
Tyndall National Institute, University College Cork, Lee Maltings, Cork, Ireland

(Received 22 March 2011; accepted 16 June 2011; published online 8 August 2011)

Size dependent current-voltage measurements were performed on InGaAs quantum dot active region mesa diodes and the surface recombination velocity was extracted from current density versus perimeter/area plots using a diffusion model. An effective surface recombination value of 5.5×10^4 cm/s was obtained that can be reduced by more than an order of magnitude by selective oxidation of $Al_{0.9}Ga_{0.1}As$ cladding layers. The values are three times smaller than those obtained for a single quantum well. The effect of p-type doping in the active region was investigated and found to increase the effective surface recombination. © *2011 American Institute of Physics*. [doi:10.1063/1.3611387]

I. INTRODUCTION

As device dimensions decrease and the surface to volume ratios increase, the role of surface recombination on the performance of devices becomes crucial.[1–4] GaAs materials have one of the worst free surfaces in solid-state electronics.[5] Surface recombination velocity values of $1–2 \times 10^5$ cm/s for InGaAs quantum wells[6,7] and 5×10^4 cm/s for quantum dots[8] (QD) have been reported in the literature. There has been no report of an electrically injected InGaAs/GaAs photonic crystal laser at room temperature yet, mainly due to high surface recombination values of GaAs. To achieve a sufficiently low surface recombination velocity for practical device applications, various surface passivation techniques have been investigated including oxide or nitride deposition, native oxide formation, coating a sodium hydroxide or sulfide film, and laser annealing.[9,10] In quantum dot materials, surface recombination effects are expected to be suppressed compared to bulk materials because of the carrier confinement in three dimensions to the dots, preventing their diffusion and interaction with recombination centers at the surface.[11] In this paper, we have characterized the surface recombination velocity in In(Ga)As/GaAs QD active media *p-i-n* mesa diodes and compared the results to that of diodes with undoped quantum wells (QW) and QDs with p-type doping in the active region. In particular, the role of confining the carrier injection into the active region of the diode by selective oxidation of the AlGaAs cladding layers was investigated and shown to be a way to reduce the role of the surface. An effective surface recombination velocity is introduced to account for the reduced carrier concentration at the etched surfaces. A diffusion model is used to calculate the reduced density at the surface. The scaling behavior of the diode current[19,20] was used to characterize the surface recombination velocity and compared with other methods in the literature.

II. DESIGN AND FABRICATION

Mesa isolated cylindrical diodes ranging in diameter from 20 to 500 μm were fabricated on self-assembled In(Ga)As quantum dots on a GaAs substrate grown by NL-Nanosemiconductor GmbH (Innolume). The basic layer structure is a separate confinement $p-i-n$ heterostructure with an active region consisting of a dot in a well structure with five stacks of self-organized InAs QDs separated by 33 nm thick GaAs spacer layers, capped with 5 nm $In_{0.15}Ga_{0.85}As$ strain-reducing quantum wells. The active region is surrounded by 10 nm $Al_{0.35}Ga_{0.65}As$ layers and by 900 nm thick *n*– and *p*–doped (1×10^{18} cm^{-3}) $Al_{0.9}Ga_{0.1}As$ cladding layers. A 200 nm thick, heavily *p*–doped (10^{20} cm^{-3}) GaAs cap layer and a 500 nm thick n^+ GaAs buffer layer were used. The interface between the AlGaAs claddings and the GaAs layers is linearly graded. The fabrication process started with the definition of p-type contact pads where Ti/Pt/Au was deposited by electron beam evaporation followed by alloying. 4.1 μm high mesas were defined by etching through the junction using inductively coupled plasma etch in BCl_3 chemistry. An Au/Ge/Ni/Au alloy was deposited on the back of the substrate as n-metal contact. Prior to metal deposition the samples were dipped in 1:1 HCl:H_2O solution briefly for better adhesion. The actual mesa sizes were measured by an optical microscope and these values were used in the calculations.

Selective oxidation of the AlGaAs cladding layers, which has been extensively used in optoelectronic device fabrication,[12–18] was investigated here as a means to reduce the influence of the surface by reducing carrier diffusion to the etched surfaces. Some of the samples were placed in an oxidation furnace after the etch step to selectively oxidize the $Al_{0.9}Ga_{0.1}As$ layers. One set of diodes were oxidized for 15 min (labeled as "sample B") and another for 30 min ("sample C") in a water vapor only ambient at 420 °C. The oxidation penetration was analyzed by cross section scanning electron microscopy (SEM) and found to be linear with a 4 μm/hour growth rate.

III. RESULTS AND DISCUSSION

The forward dark current-voltage (*I–V*) characteristics of the diodes were measured as a function of the mesa diameter using a Hewlett Packard 4156 precision semiconductor parameter analyzer. The measurements were performed at room temperature by wafer probing in a Cascade Summit 1200 station.

[a]Electronic mail: brian.corbett@tyndall.ie.

 © 2011 American Institute of Physics

Figure 1 shows the dark current density versus voltage (J–V) plots of different size diodes for the reference ("sample A"), and sample C. The insets magnify the graph area around 0.5V. Comparing the insets shows that the current density at a given voltage is significantly reduced by the oxidation. Also the larger separation between the curves for the reference sample shows that size dependence is more significant in the reference sample, suggesting a higher contribution of non-radiative perimeter current that can be explained by the following.

A. Method

Carriers injected into the active region recombine either in the bulk or at the surface. Therefore the current (I) can be expressed as the sum of bulk (I_b) and surface components (I_s), and dividing both sides by the diode area (A) gives for the current density

$$J = J_b + J_s\,(P/A), \tag{1}$$

where J_b is the bulk recombination current density and J_s is the surface recombination current per unit length of the perimeter (P).[21] Therefore plotting J versus P/A, the bulk and perimeter current contributions can be separated.

Figure 2 shows the measured current density J at 0.5 V bias, where the non-radiative recombination dominates over the radiative term while the effects of diode resistance and high injection are minimal, versus perimeter/area ratio (P/A) for the three samples. For the oxidized devices, the oxidation depth is subtracted from the mesa radii. While the bulk recombination current density extracted from the intercept is the same for all samples ($J_b = 4.1 \times 10^{-5}$ A/cm^2), the perimeter recombination current density J_s extracted from the

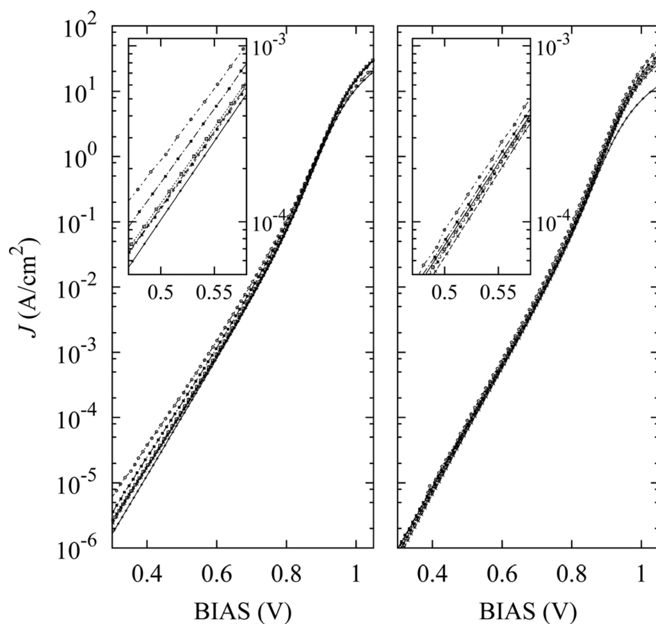

FIG. 1. Current density J of different size diodes as a function of voltage for samples A (left) and C (right). Solid lines at the bottom are for the largest size diodes (500 μm diameter) and the size decreases regularly upwards (200 μm, 150 μm, 100 μm, 50 μm, 20 μm). Insets show around 0.5 V in detail.

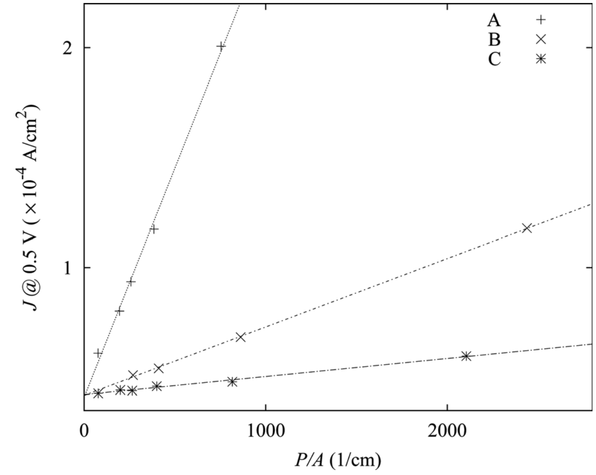

FIG. 2. Measured current density (J) at 0.5 V vs perimeter/area ratio (P/A) plot for the reference sample A, sample B (15 min oxidized), and sample C (30 min oxidized).

slope is reduced by more than an order of magnitude by the 30-min oxidation. Table I lists the extracted J_s values. This reduction in the perimeter recombination current density corresponds to a reduction in the effective surface recombination velocity as follows.

B. Diffusion model

Minority carriers diffuse to the perimeter, because of the concentration gradient created by the enhanced recombination around the surface or by the oxidized regions, and recombine there. Using the notation of Fig. 3 showing the device structure, in cylindrical coordinates this yields[22]

$$-qD\frac{\partial n}{\partial r}\bigg|_{r=R} = qU_s = S(n(R) - n_i), \tag{2}$$

where D is the diffusion coefficient, R is the radius of the mesa, and n_i is the intrinsic carrier density. U_s is the rate of surface recombination that is proportional to the excess carrier density at the surface, $(n(R) - n_i)$, with a proportionality constant S called the *surface recombination velocity*.

The perimeter recombination current per unit length is found by integrating the surface recombination current density qU_s along the direction perpendicular to the junction, over the surface of the active region (or the effective surface diffusion length (L_s), which can be approximated by the active layer thickness for thin (< 0.1 μm) active layers[23])

$$J_s = q\int_a^b U_s\,\mathrm{d}z = q(n(R) - n_i)SL_s, \tag{3}$$

TABLE I. Perimeter recombination current density and effective surface recombination velocity values extracted from J vs P/A plots for samples with different oxidation times.

Sample	Ox. time	J_s (A/cm)	S_{eff} (cm/s)	$n(R)/n(0)$
A	Ref.	2.1×10^{-7}	5.5×10^4	0.78
B	15 min	4.3×10^{-8}	1.4×10^4	0.22
C	30 min	1.7×10^{-8}	4.4×10^3	0.06

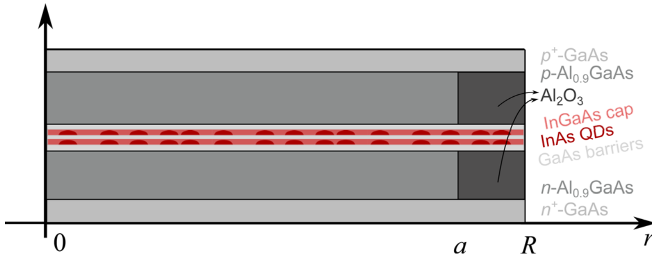

FIG. 3. (Color online) Schematics of the structure. R is the mesa radius and a is the oxidation depth coordinate.

where the carrier density at the surface is assumed to be constant along the surface of the active region. Multiplying and dividing by the excess carrier density in the bulk $(n(0) - n_i)$ and using $n(0) = n_i \exp(qV/\eta kT)$, the saturation part of the above equation for current density can be written as

$$J_{s0} = qn_i S_{eff} L_s, \tag{4}$$

where $S_{eff} \equiv S \cdot (n(R) - n_i)/(n(0) - n_i)$ is the effective surface recombination velocity. Therefore, the perimeter recombination current density is directly proportional to the effective surface recombination velocity. Thus, the change in perimeter recombination current density extracted from the slope of Fig. 2 also implies a change in the effective surface recombination velocity by the same rate.

Taking the intrinsic carrier density of $In_{0.15}Ga_{0.85}As$ at 300 K as[24] $n_i = 1.3 \times 10^8$ cm^{-3} and the active layer thickness as $L_s = 5 \times 5.8 = 29$ nm (5 QD stack with 5 nm InGaAs layer and 0.8 nm InAs) effective surface recombination values are calculated and listed in Table I. The effective surface recombination velocity of reference sample A is found to be $S_{eff} = 5.5 \times 10^4$ cm/s, which is reduced to 4.4×10^3 cm/s for sample C by 30 min oxidation. The last column is the excess carrier density at the surface of the device relative to the value at the center.

The carrier density at the surface can be obtained theoretically by solving the diffusion equation describing the transport of minority carriers in cylindrical coordinates for the given boundary conditions

$$\frac{n(r) - n_i}{n(0) - n_i} = \begin{cases} 1 - \dfrac{K_{1a} - I_{1a}/M}{I_{0a}K_{1a} + I_{1a}K_{0a}} I_0(r/L) & r < a, \\ \dfrac{I_{1a}}{I_{0a}K_{1a} + I_{1a}K_{0a}} (I_0(r/L)/M + K_0(r/L)) & a < r < R, \end{cases} \tag{5}$$

where a is the radius of the unoxidized part of the device, I_n and K_n are the modified Bessel functions of the first and second kinds of nth order, and M is a constant for a given radius R given by $M = (v\, I_{1R} + S\, I_{0R})/(v\, K_{1R} - S\, K_{0R})$, where v is the diffusion velocity. The notation $I_n(x/L) \equiv I_{nx}$ is adopted to simplify repeating long arguments and the same applies to K.

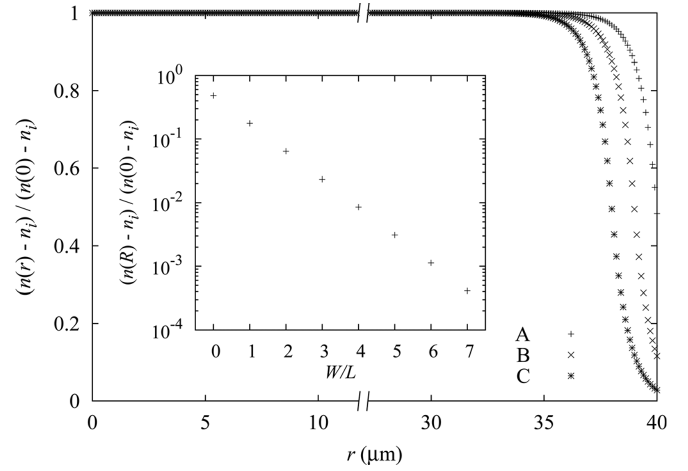

FIG. 4. Calculated relative steady state minority carrier distribution for the reference sample A, sample B (15 min oxidized), and sample C (30 min oxidized). Inset shows relative excess carrier density at the surface as a function of relative oxidation depth (W/L).

This solution for a diode with radius $R = 40$ μm is plotted in Fig. 4 for different values of oxidation depth. $D = 20$ cm^2/s, $\tau = 0.3$ ns are the values used for the diffusion coefficient and lifetime.[25–27] The diffusion length and velocity are calculated from these values as $L = 0.7$ μm and $v = 2.6 \times 10^5$ cm/s. An iterated surface recombination velocity value of $S = 7 \times 10^4$ cm/s gives the ratio of the excess carrier density at the surface to the one in the bulk for samples A, B, and C as 0.78, 0.22, and 0.06, respectively, which fits best with the observed reduction in effective surface recombination values (Table I).

An expression relating the excess carrier density at the surface to the oxidation depth ($W = R - a$) is obtained by substituting $r = R$ in Eq. (5)

$$\frac{n(R) - n_i}{n(0) - n_i} = \frac{I_{0R}K_{1R} + I_{1R}K_{0R}}{I_{0a}K_{1a} + I_{1a}K_{0a}} \cdot \frac{I_{1a}}{I_{1R} + (S/v)I_{0R}}, \tag{6}$$

which is plotted in the inset of Fig. 4 showing that the excess carrier density at the surface decays exponentially with increasing oxidation depth.

C. *p*-doping and QW comparisons

p-type doping of the GaAs spacer layers in the active region is used to improve the temperature performance and the modulation bandwidth of QD lasers.[28] The effect of this p-doping on the surface recombination was investigated here. In this case the number of dot layer stacks was 10 in the material structure, and the GaAs spacer layers between the dots were p-doped. Mesa isolated diode structures with a range of different sizes were fabricated as previously described but without oxidation. Figure 5 plots dark current density versus voltage plots of the different size diodes for the p-type doped sample. Comparing the inset that is the detailed view around 0.5 V to the inset of Fig. 1 with same scales for samples A and C, it is seen that current density of the p-type doped sample is higher than the undoped sample's at the same voltage levels.

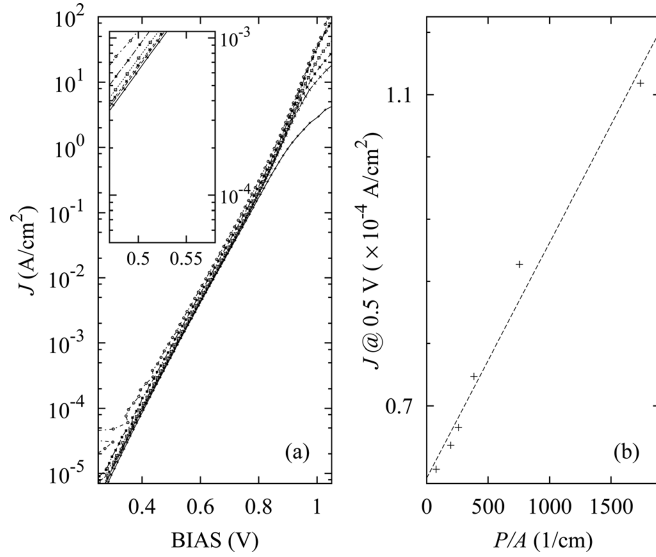

FIG. 5. Current density J of different size diodes as a function of voltage for the sample with p-type doped GaAs barrier layers. (b) Extracted current density at 0.5 V vs P/A ratio plot for that sample.

Figure 5 (right) shows the measured current density J at 0.5 V bias, for different size diodes versus perimeter/area ratio. The bulk recombination current density extracted from the intercept of the linear fit to data is $J_b = 6.1 \times 10^{-4}$ A/cm^2, and the perimeter recombination current density extracted from the slope is $J_s = 3.0 \times 10^{-7}$A/cm. Calculating the effective surface recombination value from the J_s value we get $S_{eff} = 1.6 \times 10^5$ cm/s. Compared to the undoped structures, the higher value of surface recombination velocity for structures with p-doped barriers can be explained as follows.

The rate of surface recombination U_s in Eq. (2), the number of carriers recombining at the surface per unit area per unit time, describing the kinetics of surface recombination is given by the results of Shockley-Read and Hall

$$U_s = \sigma v N_t \frac{n_s p_s - n_i^2}{n_s + p_s + 2n_i}, \tag{7}$$

where N_t is the density of recombination centers, σv is the capture cross section-thermal velocity product, and n_s,p_s denotes the electron and hole carrier concentrations at the surface. Defining the product $\sigma v N_t$, with dimensions centimeters per second, as s_0 and taking $p_s = n_s$ for intrinsic active materials, this gives

$$U_s = s_0/2\,(n_s - n_0). \tag{8}$$

Comparing that with Eq. (2) again, the surface recombination velocity is given by $S = s_0/2 = \sigma v N_{st}$.

For the sample with the p-doped GaAs barrier layers in the active layer, the picture is a bit different. The hole concentration in the barrier layers is equal to the doping concentration ($N_A = 5 \times 10^{17}$ cm^{-3}), which will also diffuse into the well layers and the QDs because of their small dimensions compared to diffusion length scales. Therefore, taking $p \simeq N_A$ for low-level injection and using $n_0 N_A = n_i^2$, recombination rate for sample with p-doped barriers is given by

$$U_s = s_0 \frac{N_A}{n_s + p_s + 2n_i}(n_s - n_0). \tag{9}$$

Using also the fact that $N_A \gg n$, n_i for low-level injection we get $S \simeq s_0$. Therefore, surface recombination velocity in the p-doped sample was expected and found to be higher than for the undoped samples.

Finally, to compare with quantum wells, devices were fabricated on a 7 nm single $In_{0.11}Ga_{0.89}As$ layer active region quantum well wafer with a peak emission at around 980 nm. The effective surface recombination value calculated by a similar analysis for the single quantum well is found to be $S_{eff} = 1.6 \times 10^5$ cm/s, about three times higher than the value when quantum dots are incorporated in the active region.

IV. SUMMARY AND CONCLUSION

In conclusion, surface recombination on In(Ga)As/GaAs quantum dot active region mesa diodes was investigated by simple size dependent current-voltage measurements. A low effective surface recombination value of 5.5×10^4 cm/s and an iterated surface recombination velocity value of $S = 7 \times 10^4$ cm/s were obtained agreeing well with values in the literature found by other methods. More than an order of magnitude reduction in the effective surface recombination velocity is achieved by selective oxidation of $Al_{0.9}Ga_{0.1}As$ cladding layers. This is due to the effectiveness of the oxidation in reducing the minority carrier density at the surface. Compared to a single InGaAs quantum well, these surface recombination values are about three times smaller. The effect of p-type doping in the active region was also investigated and found to increase surface recombination. To summarize, surface recombination in In(Ga)As/GaAs quantum dot active region mesa diodes are lower compared to quantum wells as expected due to carrier confinement by dots. Further reductions can be achieved by keeping the carriers away from the surface by oxidizing the claddings, while p-doping the active region can increase it.

ACKNOWLEDGMENTS

This study was supported by the Science Foundation Ireland through the National Access Programme.

[1] M. Francardi, L. Balet, A. Gerardino, N. Chauvin, D. Bitauld, L. H. Li, B. Alloing, and A. Fiore, Appl. Phys. Lett. **93**, 143102 (2008).
[2] D. Englund, H. Altuğ, and J. Vučković, Appl. Phys. Lett. **91**, 071124 (2007).
[3] S. Tanriseven, P. Maaskant, and B. Corbett, Appl. Phys. Lett. **92**, 123501 (2008).
[4] O. Demichel, M. Heiss, J. Bleuse, H. Mariette, and A. Fontcubertai Morral, Appl. Phys. Lett. **97**, 201907 (2010).
[5] E. Yablonovitch and R. Bhat, Appl. Phys. Lett. **60**, 371 (1992).
[6] S. Y. Hu, S. W. Corzine, K. Law, D. B. Young, A. C. Gossard, L. A. Coldren, and J. L. Merz, J. Appl. Phys. **76**, 4479 (1994).
[7] X. Xu, T. Yamada, and A. Otomo, Appl. Phys. Lett. **92**, 091911 (2008).
[8] S. Moore, L. O'Faolain, M. Cataluna, M. Flynn, M. Kotlyar, and T. Krauss, IEEE Photon. Technol. Lett. **18**, 1861 (2006).
[9] C. K. Chia, M. Suryana, and M. Hopkinson, Appl. Phys. Lett. **95**, 141106 (2009).
[10] E. Yablonovitch and T. J. Gmitter, U.S. patent 4843037 (June 27, 1989).
[11] A. Fiore, M. Rossetti, B. Alloing, C. Paranthoen, J. X. Chen, L. Geelhaar, and H. Riechert, Phys. Rev. B **70**, 205311 (2004).
[12] W. T. Tsang, Appl. Phys. Lett. **33**, 426 (1978).

[13]J. M. Dallesasse, N. Holonyak, Jr., A. R. Sugg, T. A. Richard, and N. El-Zein, Appl. Phys. Lett. **57**, 2844 (1990).
[14]F. A. Kish, S. J. Caracci, N. Holonyak, Jr., J. M. Dallesasse, K. C. Hsieh, and M. J. Ries, Appl. Phys. Lett. **59**, 1755 (1991).
[15]K. D. Choquette, K. M. Geib, H. C. Chui, B. E. Hammons, H. Q. Hou, T. J. Drummond, and R. Hull, Appl. Phys. Lett. **69**, 1385 (1996).
[16]K. D. Choquette, K. M. Geib, C. I. H. Ashby, R. D. Twesten, O. Blum, H. Q. Hou, D. M. Follstaedt, B. E. Hammons, D. Mathes, and R. Hull, Quantum Electron. **3**, 916 (1997).
[17]H. Gebretsadik, K. Zhang, K. Kamath, X. Zhang, and P. Bhattacharya, Appl. Phys. Lett. **71**, 3865 (1997).
[18]A. Fiore, J. X. Chen, and M. Ilegems, Appl. Phys. Lett. **81**, 1756 (2002).
[19]B. Corbett and W. M. Kelly, Appl. Phys. Lett. **62**, 87 (1993).
[20]C. Kelleher, R. Ginige, B. Corbett, and G. Clarke, Appl. Phys. Lett. **85**, 6033 (2004).
[21]V. Swaminathan, J. M. Freund, L. M. F. Chirovsky, T. D. Harris, N. A. Kuebler, and L. A. D'Asaro, J. Appl. Phys. **68**, 4116 (1990).
[22]A. S. Grove, *Physics and Technology of Semiconductor Devices* (Wiley, New York, 1967).
[23]C. H. Henry, R. A. Logan, and F. R. Merritt, J. Appl. Phys. **49**, 3530 (1978).
[24]S. Paul, J. B. Roy, and P. K. Basu, J. Appl. Phys. **69**, 827 (1991).
[25]V. Malyarchuk, J. W. Tomm, V. Talalaev, C. Lienau, F. Rinner, and M. Baeumler, Appl. Phys. Lett. **81**, 346 (2002).
[26]G. Raino, A. Salhi, V. Tasco, M. D. Vittorio, A. Passaseo, R. Cingolani, M. D. Giorgi, E. Luna, and A. Trampert, J. Appl. Phys. **103**, 096107 (2008).
[27]C. Zinoni, B. Alloing, C. Monat, V. Zwiller, L. H. Li, A. Fiore, L. Lunghi, A. Gerardino, H. de Riedmatten, H. Zbinden, and N. Gisin, Appl. Phys. Lett. **88**, 131102 (2006).
[28]O. B. Shchekin and D. G. Deppe, Appl. Phys. Lett. **80**, 3277 (2002).